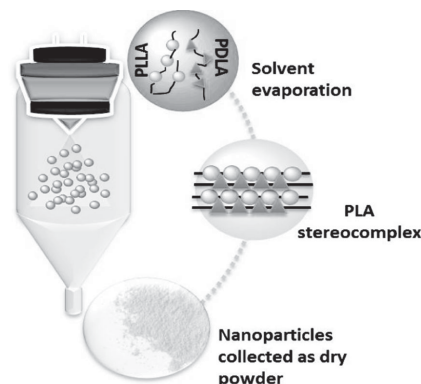


# Nano-Stereocomplexation of Polylactide (PLA) Spheres by Spray Droplet Atomization

Veluska Arias, Karin Odelius, Ann-Christine Albertsson\*

A direct, efficient, and scalable method to prepare stereocomplexed polylactide (PLA)-based nanoparticles (NPs) is achieved. By an appropriate combination of fabrication parameters, NPs with controlled shape and crystalline morphology are obtained and even pure PLA stereocomplexes (PLASC) are successfully prepared using the spray-drying technology. The formed particles of varying D- and L-LA content have an average size of  $\approx 400$  nm, where the smallest size is obtained for PLA50, which has an equimolar composition of PLLA and PDLA in solution. Raman spectra of the particles show the typical shifts for PLASC in PLA50, and thermal analysis indicates the presence of pure stereocomplexation, with only one melting peak at 226 °C. Topographic images of the particles exhibit a single phase with different surface roughness in correlation with the thermal analysis. A high yield of spherically shaped particles is obtained. The results clearly provide a proficient method for achieving PLASC NPs that are expected to function as renewable materials in PLA-based nanocomposites and potentially as more stable drug delivery carriers.



## 1. Introduction

“Magic bullets,” Ehrlich’s concept of small particles that could deliver active molecules to a specific site in the body, is still the principal driving force for nanoparticle (NP) development. NPs are not only attractive for the pharmaceutical field but also serve as reinforcements in high-performance materials. NPs can be produced by several methods, such as emulsion evaporation, solvent displacement, and emulsification diffusion. Among the solvent displacement methods, spray-drying has been used for many years as a technique for producing particles with regular

size and morphology for different applications.<sup>[1]</sup> The advantages of the spray-drying technique include a simple and one-step approach to obtain particles in dry form, narrow particle size distribution, high yields directly from solution, scale-up capability, and low-energy consumption. Therefore, spray-drying has become an attractive method to create particles from different types of polymeric solutions<sup>[2]</sup> and is potentially applicable in the production of more sophisticated particles involving polymer complexes.

Stereocomplex (SC) formation in polymers is the association of pairs of optically active *S*- or *R*-polymers (*l*- and *d*-polymer forms) or between optically inactive syndiotactic and isotactic polymers. The stereoselective association depends on structural fitting and on the van der Waals forces between polymer chains.<sup>[3]</sup> SC in polymers has been reported between enantiomeric polylactides (PLAs),<sup>[4]</sup> isotactic and syndiotactic poly(methyl methacrylate)s (PMMA)s,<sup>[5]</sup> and enantiomeric poly(2-hydroxybutyrate)s (PHBs).<sup>[6]</sup>

The SC of optically active PLA has a melting temperature ( $T_m$ ) between 210 and 230 °C, approximately

V. Arias, Dr. K. Odelius, Prof. A.-C. Albertsson  
Department of Fibre and Polymer Technology, KTH Royal  
Institute of Technology, SE-100 44 Stockholm, Sweden  
E-mail: aila@polymer.kth.se

This is an open access article under the terms of the Creative Commons Attribution-NonCommercial-NoDerivs License, which permits use and distribution in any medium, provided the original work is properly cited, the use is non-commercial and no modifications or adaptations are made.

50 °C higher than that of the polymer of the pure enantiomeric form, and with a different organization of the crystalline lattice.<sup>[7]</sup> Recent work has explored developing a PLA stereocomplex (PLASC) by crystallization of block copolymers,<sup>[4b,8]</sup> casting of films from concentrated solutions,<sup>[4c,d]</sup> melt blending processes,<sup>[4e,9]</sup> layer-by-layer deposition,<sup>[4f]</sup> electrospinning,<sup>[4g]</sup> and suspensions in organic solutions.<sup>[4h,10]</sup> PLASCs are formed from solution, in bulk state from the melt, during polymerization, and during degradation as long as L-lactyl and D-lactyl units with the required length<sup>[11]</sup> coexist in the system. The final physical and thermomechanical properties of the SC are highly dependent on both the degree of crystallinity and solid-state morphology. We have previously reported several methods to improve the limited thermomechanical properties of the quite commercially attractive PLA polymers.<sup>[12]</sup> Thus, the underlying reason for the large amount of interest in PLASC is its potential as an efficient solution to improve the properties of PLA, particularly thermal and hydrolysis resistance.<sup>[13]</sup> NPs of PLASC have been shown to enhance the mechanical and thermal stability of the host matrix.<sup>[14]</sup> However, the preparation of NPs currently involves complicated methods whereby surfactants or other adjuvants may remain in the particles after formation, usually resulting in a low yield of production.<sup>[15]</sup> Previous methods have focused on the SC formation in PLA without considering reproducibility and future scalability. Therefore search for controllable, high-yield, and less-expensive systems continues.

Our goal was to generate a controllable, scalable, and economical method to prepare NPs of PLA SC. To achieve this, we have focused on an already industrially established technology, namely spray drying. This process provides a direct approach to induce the formation of particles with controlled shape in a high-yield production, and thus should open the possibility for NPs formation. Our hypothesis was that, by screening PLA solutions in a wide range of concentrations, crystallization would occur under specific atomization and solvent evaporation conditions, leading to the formation of PLA particles with precise crystalline and morphological structures.

## 2. Results and Discussion

The preparation of PLASC NPs by the spray-drying technique from enantiomeric PLA organic solutions was performed as depicted in Figure 1. The systems selected for particle formation permitted a comprehensive view of PLASC formation by the atomization process. Solutions consisting of pure PLLA, PDLA, PLA75 (PLLA/PDLA in a ratio of 75/25), and PLA50 (equimolar solution of PLLA and PDLA) were used. The variation of polymer concentration in the PLA solutions led to the gradual formation of pure

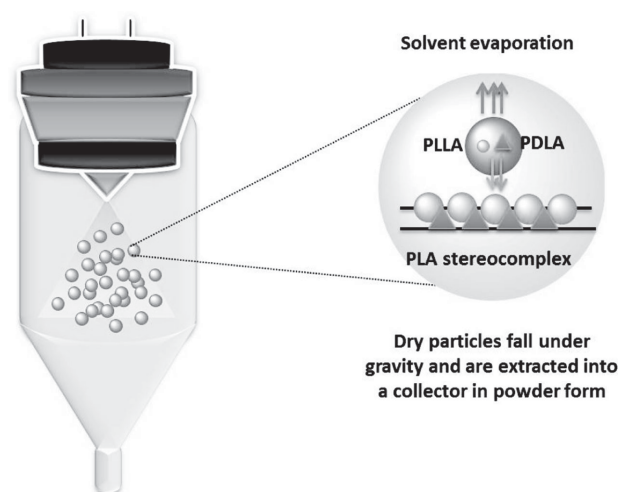


**Figure 1.** Schematic representation of PLASC formation by spray-drying. PLA solutions (0.25 g/100 mL) in chloroform were pumped into the spray-dryer and directly atomized into fine droplets by forcing the fluid through a pressure nozzle. The droplets were then subjected to a very fast drying process and finally collected as a dry powder.

SC crystallites. After atomization, the droplet converts into the dry particle form by solvent evaporation under an inert atmosphere. The speed of solvent evaporation depends on the temperature and flow of the carrier gas.

SC formation does not occur merely by mixing equimolarly diluted PLLA and PDLA solutions. Stereoselective association occurs during solvent evaporation due to changes in the solution concentration. Here, it is demonstrated that, under a rapid solvent evaporation rate, pure SC crystallites are formed. SC has long been known to occur when the solvent evaporation rate is sufficiently slow, as a rapid rate of evaporation will not provide sufficient time for SC crystallite formation; thus, the polymer concentration instead reaches the critical level of homocrystallization, which is the case when inducing SC from solution casting where a rapid solvent evaporation results in two types of crystal populations.<sup>[7a]</sup> Upon solvent evaporation, the polymer concentration first reaches the critical level of SC crystallite formation and then that of homocrystallite formation. During the spray-drying process, solvent evaporation occurs at such an elevated rate that there is no time for homocrystallites to form, which is translated as SC crystallites forming predominantly in equimolar solutions of PLLA and PDLA. PLA racemic crystallization, that is, SC, takes place more readily than homocrystallization, which is explained by its occurrence at lower polymer concentrations than for homocrystallization. This corroborates the suggestion that SC formation is thermodynamically more favorable than homocrystallization.<sup>[16]</sup> Throughout the spray-drying, as the solvent evaporation rate is fast, there is a rapid increase in the polymer concentration. The high

density of SC crystallites that are initially formed act as nuclei for new SC crystallites under the increasing density of tie polymer chains with the increment of polymer concentration. This is explained by the intermolecular crystallization, which dominates in SC formation in equimolar solution of PLLA and PDLA upon solvent evaporation. Intermolecular crystallization causes an increase of the tie chains between the crystallites.<sup>[17]</sup>

During atomization, the droplet formation occurs immediately after the polymer solution passes through the nozzle. The surface area per unit increases, which raises the probability of interaction between PLLA and PDLA chain segments. These conditions enhance SC crystallite formation and increases the degree of crystallinity ( $\chi_c$ ) and melting temperature ( $T_m$ ) of PLA above those of PLA composed of pure homocrystallites. The molar mass of the polymers also affects the formation of SC crystallites in equimolar mixtures of PDLA and PLLA in solution. PLA polymers with high molar mass are required for mechanical performance. Here, PLA with pure SC crystallites were produced with polymers having a molar mass over 150 kDa (Table 1). Previous findings report that large hydrodynamic volume of PDLA and PLLA molecules retards SC crystallite formation, resulting in a large number of homocrystallites.<sup>[18]</sup> In this case, the high molar mass increases the nuclei density of crystallites formation during the solvent evaporation enhancing the SC formation.<sup>[17]</sup> The sizes of the particles obtained for PLLA and PDLA were all in the same range. Interestingly, SC particles were smaller in size due to the secondary forces between L-lactyl and D-lactyl units that influence particle size upon solvent evaporation. During SC formation, L- and D-chains have a particularly strong interaction where the chains are packed side-by-side, giving rise to a more dense packing of the crystalline structure.<sup>[19]</sup> The particle production yield (PPY) varied between 60% and 70% for all particles, confirming the efficacy of the technique for producing small particles in a single batch with high yield.<sup>[20]</sup>

Directly after the particles production, FT-Raman spectroscopy was performed to assure the SC formation

before thermal analysis. SC is often traced by differential scanning calorimetry (DSC); however, the crystallinity obtained could be a combination of the induced crystallization from the DSC method and the true crystallinity of the sample leading to uncertain results. The driving force for the nucleation of PLA SC crystallites, first reported by Zhang et al., was explained by hydrogen bonding between the methyl groups and carbonyl oxygen in the chains.<sup>[21]</sup> In PLAs, O=C stretching is sensitive to variations in morphology and conformation. Spectroscopic differences were observed between the particle systems due to differences in helical conformations (Figure 2). The Raman line observed in PLLA assigned to the  $\nu\text{C}=\text{O}$  stretching mode was split into components observed at 1758, 1766, and 1772  $\text{cm}^{-1}$ . For PDLA, the  $\nu\text{C}=\text{O}$  stretching mode was split into components observed at 1757, 1768, and 1773  $\text{cm}^{-1}$ , respectively. In the spectrum of PLA75, the Raman lines were broad and asymmetric, showing two components at 1772 and 1752  $\text{cm}^{-1}$ . This behavior is due to pair addition mechanisms, commonly observed in less crystalline PLA materials.<sup>[22]</sup> In the case of PLA50, the spectrum showed a shift in the sharp peak observed at 1751  $\text{cm}^{-1}$ , with a broad diffusion band assigned to the characteristic  $\nu\text{C}=\text{O}$  stretching of the PLASC.<sup>[21,23]</sup>

Thermal analysis of the particles (Figure 2) showed that the glass transition temperature ( $T_g$ ) and  $T_m$  increased during SC formation. PLLA and PDLA particles had a  $T_g$  of 56 and 57 °C and  $T_m$  of approximately 176 and 173 °C, respectively. PLA75 presented two melting peaks at 162 and 216 °C, corroborating the presence of racemic crystallization and homocrystallization during particle formation. Not only SCs were formed but also crystals with lower  $T_m$ , most likely from the most abundant PLLA component. PLA50 exhibited a single melting peak at 226 °C, representing the formation of pure SC or racemic crystals. These findings are in agreement with the literature, in which an equimolar mixture of PLLA and PDLA favors crystal stereocomplexation.<sup>[3a]</sup> Cold crystallization was observed for all particles. However, a small shoulder or exothermic peak was observed before the melting peak for the pure PLLA and PDLA samples. Ohtani et al.<sup>[24]</sup> concluded that, for PLA, the exothermic peak at low temperature upon heating is due to cold crystallization, and the second exothermic peak at higher temperature before the melting peak occurs due to a phase transition from the  $\beta$ -form to a more stable  $\alpha$ -form. When crystallization occurs at higher temperatures, as for PLA75 and PLA50, no such phase transition was observed. Indicative  $\chi_c$  values were obtained for all samples from thermal analysis measurements. The particles presented  $\chi_c$  of 57% and 52% for pure PLLA and PDLA, respectively. Variation in the concentration of L-lactyl and D-lactyl units in PLA75 gave a total  $\chi_c$  value of 38%, taking into consideration the contribution of both the SC and homocrystallites formed. There

**Table 1.** Molar mass of the PLA materials before the spray-drying process, particle size, and dispersity after atomization, and particle production yield.

Sample	$\bar{M}_n$ <sup>a)</sup> [Da × 10 <sup>5</sup> ]	$\bar{D}$ <sup>a)</sup>	Particle size <sup>b)</sup> [nm]	PDI <sup>b)</sup> [nm]	PPY <sup>c)</sup> [%]
PLLA	1.6 ± 0.07	1.2 ± 0.0	443.4	0.2	63
PDLA	1.8 ± 0.05	1.1 ± 0.0	435.1	0.2	65
PLA75	–	–	425.7	0.2	70
PLA50	–	–	364.8	0.2	66

<sup>a)</sup>Determined by SEC; <sup>b)</sup>z-average value; <sup>c)</sup>Particle production yield determined by gravimetry.

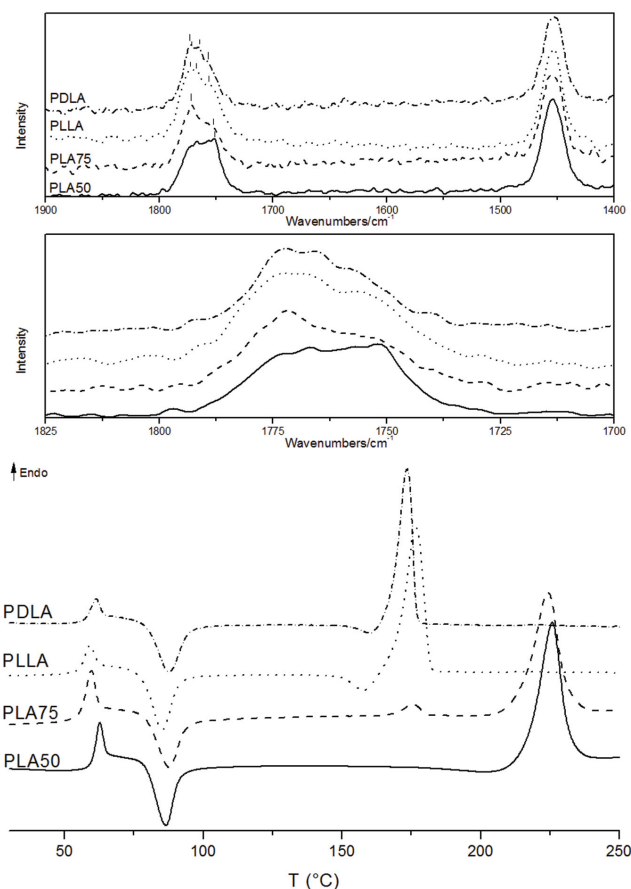


**Figure 2.** Top: Raman spectra of PLLA, PDLA, PLA75, and PLA50 particles, with close look of the tacticity-sensitive band (1825–1700  $\text{cm}^{-1}$  region). Bottom: DSC thermograms of the 1<sup>st</sup> heating scan of particle systems PLLA, PDLA, PLA50, and PLA75, directly after particle formation.

is a decrease in  $\chi_c$  due to the disorder introduced by the D-units in a polymer rich with L-units. When reaching the equimolar concentration of L-lactyl and D-lactyl units in PLA50,  $\chi_c$  was again 56%, demonstrating the formation of pure SC crystallites.

The topographies of the particles were analyzed using tapping-mode imaging in atomic force microscopy (AFM) (Figure 3); the root-mean-square roughness ( $R_q$ ) of the surfaces was calculated using three representative topographical images of each sample. All particles showed one uniform phase, with different surface roughnesses for each material. These differences in the roughness are possibly due to the variances in the crystallinity of the samples, as indicated in thermal analysis measurements. The morphology of the particle surfaces (Figure 3) shows that small spherical particles were obtained in all cases by the spray-drying technique. In all cases, dispersity in the particle size was observed. In the spray-dryer, the droplets are subjected to a turbulent gas flow through the chamber, which leads to differences in drying degree,

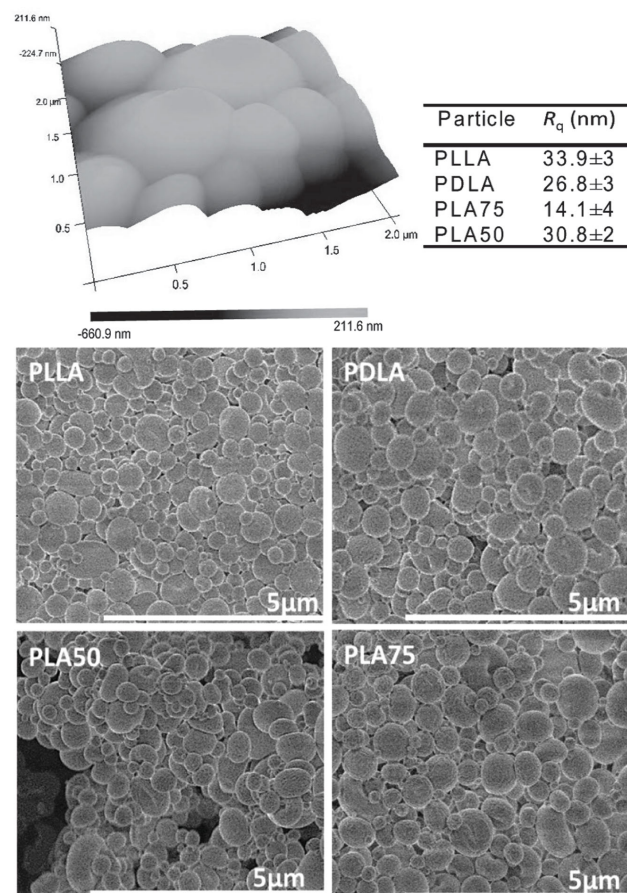


**Figure 3.** Top: Representative AFM height image of PLA50. All AFM images were scanned over a  $2 \times 2 \mu\text{m}^2$  area. Bottom: SEM images of PLA particle systems.

and hence, a slight non-homogeneity in particle size and morphology can be obtained. Here, in all cases, the major population showed homogeneous size distribution and spherical shape.

### 3. Conclusions

An efficient method to obtain biodegradable NPs of PLASC by spray-drying atomization was successfully achieved with well-defined parameters. Spherical particles in the nanosize range were obtained in high yield for all systems. Pure SC crystallites in the PLA NPs were formed at a specific polymeric solution concentration and defined atomization and solvent evaporation conditions. The best formulation was obtained when PLLA and PDLA polymers with a molar mass of ca.  $1.8 \times 10^5$  Da were in an equimolar ratio in the solution. Raman and thermal properties of the particles confirmed that, for solutions of pure PLLA and PDLA, homocrystallization occurs. In the case of the non-equimolar solution PLA75, SC crystallization and homocrystallization occurred during solvent evaporation.

The equimolar PLA50 solution shows pure racemic or SC crystallization during solvent evaporation. Homocrystallization was observed when the concentration of PDLA and PLLA in the solution deviates from the 0.5 level. Crucial parameters that affect SC formation are the mixing ratio and molar mass of the L-lactyl and D-lactyl units. These findings suggest production scalability of NPs of PLASC for advanced material formulations.

## Supporting Information

Supporting Information is available from the Wiley Online Library or from the author.

**Acknowledgements:** The authors acknowledge the Swedish Research Council, VR (grant ID: 62120134081) and the ERC Advance Grant, PARADIGM (grant agreement No.: 246776) for their financial support of this work.

Received: July 3, 2014; Revised: August 4, 2014;  
Published online: September 29, 2014; DOI: 10.1002/marc.201400374

**Keywords:** biodegradable; nanoparticles; polylactides; spray-drying; stereocomplexes

- [1] R. Vehring, W. R. Foss, D. Lechuga-Ballesteros, *J. Aerosol Sci.* **2007**, *38*, 728.
- [2] a) M. C. I. M. Amin, A. G. Abadi, H. Katas, *Carbohydr. Polym.* **2014**, *99*, 180; b) A. D. Patel, A. Agrawal, R. H. Dave, *J. Pharm. Sci.* **2013**, *102*, 1847; c) B. Bittner, K. Mäder, C. Kroll, H. H. Borchert, T. Kissel, *J. Controlled Release* **1999**, *59*, 23.
- [3] a) H. Tsuji, S. H. Hyon, Y. Ikada, *Macromolecules* **1991**, *24*, 5651; b) D. Brizzolara, H.-J. Cantow, K. Diederichs, E. Keller, A. J. Domb, *Macromolecules* **1996**, *29*, 191; c) H. Tsuji, H. Matsuoka, *Macromol. Rapid Commun.* **2008**, *29*, 1372.
- [4] a) Y. Ikada, K. Jamshidi, H. Tsuji, S. H. Hyon, *Macromolecules* **1987**, *20*, 904; b) H. Tsuji, Y. Ikada, *Macromolecules* **1992**, *25*, 5719; c) J. Shao, J. Sun, X. Bian, Y. Cui, Y. Zhou, G. Li, X. Chen, *Macromolecules* **2013**, *46*, 6963; d) L. Calucci, C. Forte, S. J. Buwalda, P. J. Dijkstra, *Macromolecules* **2011**, *44*, 7288; e) R. Ramy-Ratiarison, V. Lison, J.-M. Raquez, E. Duquesne, P. Dubois, *Green Chem.* **2014**, *16*, 1759; f) T. Akagi, T. Fujiwara, M. Akashi, *Langmuir* **2014**, *30*, 1669; g) M. Spasova, N. Manolova, D. Paneva, R. Mincheva, P. Dubois, I. Rashkov, V. Maximova, D. Danchev, *Biomacromolecules* **2010**, *11*, 151; h) M. Brzezinski, T. Biedron, A. Tracz, P. Kubisa, T. Biela, *Macromol. Chem. Phys.* **2014**, *215*, 27.
- [5] T. Miyamoto, H. Inagaki, *Polym. J.* **1970**, *1*, 46.
- [6] H. Tsuji, M. Hosokawa, Y. Sakamoto, *ACS Macro Lett.* **2012**, *1*, 687.
- [7] a) H. Tsuji, *Macromol. Biosci.* **2005**, *5*, 569; b) J. M. Becker, R. J. Pounder, A. P. Dove, *Macromol. Rapid Commun.* **2010**, *31*, 1923.
- [8] J. Łukaszczyk, P. Jelonek, B. Trzebicka, J. Domb Abraham, in *e-Polymers*, Vol. 10, De Gruyter, Berlin, Germany **2013**, 798.
- [9] a) S. C. Schmidt, M. A. Hillmyer, *J. Polym. Sci., Part B: Polym. Phys.* **2001**, *39*, 300; b) Y. Furuhashi, Y. Kimura, H. Yamane, *J. Polym. Sci., Part B: Polym. Phys.* **2007**, *45*, 218.
- [10] T. Biedroń, M. Brzeziński, T. Biela, P. Kubisa, *J. Polym. Sci., Part A: Polym. Chem.* **2012**, *50*, 4538.
- [11] S. J. de Jong, W. N. E. Van Dijk-Wolthuis, J. J. Kettenes-van den Bosch, P. J. W. Schuyf, W. E. Hennink, *Macromolecules* **1998**, *31*, 6397.
- [12] a) V. Arias, A. Höglund, K. Odellius, A.-C. Albertsson, *J. Appl. Polym. Sci.* **2013**, *130*, 2962; b) V. Arias, A. Höglund, K. Odellius, A.-C. Albertsson, *Biomacromolecules* **2014**, *15*, 391; c) S. R. Andersson, M. Hakkarainen, A.-C. Albertsson, *Polymer* **2013**, *54*, 4105.
- [13] a) S. R. Andersson, M. Hakkarainen, S. Inkinen, A. So-dergård, A.-C. Albertsson, *Biomacromolecules* **2010**, *11*, 1067; b) R. Slivniak, A. J. Domb, *Biomacromolecules* **2002**, *3*, 754.
- [14] R. Mincheva, P. Leclere, Y. Habibi, J. M. Raquez, P. Dubois, *J. Mater. Chem. A* **2014**, *2*, 7402.
- [15] D. Quintanar-Guerrero, E. Allemann, H. Fessi, E. Doelker, *Drug Dev. Ind. Pharm.* **1998**, *24*, 1113.
- [16] H. Tsuji, F. Horii, S. H. Hyon, Y. Ikada, *Macromolecules* **1991**, *24*, 2719.
- [17] H. Tsuji, Y. Ikada, *Polymer* **1999**, *40*, 6699.
- [18] H. Tsuji, Y. Ikada, *Stereocomplexation Between Enantiomeric Poly(lactide)s in Biodegradable Polymer Blends and Composites from Renewable Resources* (Ed.: L. Yu), John Wiley & Sons, Inc., Hoboken, NJ, USA **2009**, 163.
- [19] H. Tsuji, Y. Tezuka, *Biomacromolecules* **2004**, *5*, 1181.
- [20] A. Grenha, B. Seijo, C. Remuñán-López, *Eur. J. Pharm. Sci.* **2005**, *25*, 427.
- [21] J. Zhang, H. Sato, H. Tsuji, I. Noda, Y. Ozaki, *Macromolecules* **2005**, *38*, 1822.
- [22] G. Kister, G. Cassanas, M. Vert, *Polymer* **1998**, *39*, 267.
- [23] S. Li, M. Vert, *Macromolecules* **2003**, *36*, 8008.
- [24] Y. Ohtani, K. Okumura, A. Kawaguchi, *J. Macromol. Sci., Part B* **2003**, *42*, 875.